WATER RESOURCES RESEARCH, VOL. 50, 1–16, doi:10.1002/2013WR014073, 2014

Lithologic influences on groundwater recharge through incised glacial till from profile to regional scales: Evidence from glaciated Eastern Nebraska

John B. Gates,[1] Gregory V. Steele,[2] Paolo Nasta,[1] and Jozsef Szilagyi[3,4]

Received 3 May 2013; revised 11 December 2013; accepted 18 December 2013.

[1] Variability in sediment hydraulic properties associated with landscape depositional and erosional features can influence groundwater recharge processes by affecting soil-water storage and transmission. This study considers recharge to aquifers underlying river-incised glaciated terrain where the distribution of clay-rich till is largely intact in upland locations but has been removed by alluvial erosion in stream valleys. In a stream-dissected glacial region in eastern Nebraska (Great Plains region of the United States), recharge estimates were developed for nested profile, aquifer, and regional scales using unsaturated zone profile measurements (matric potentials, Cl^- and ^3H), groundwater tracers (CFC-12 and SF_6), and a remote sensing-assisted water balance model. Results show a consistent influence of till lithology on recharge rates across nested spatial scales despite substantial uncertainty in all recharge estimation methods, suggesting that minimal diffuse recharge occurs through upland glacial till lithology whereas diffuse recharge occurs in river valleys where till is locally absent. Diffuse recharge is estimated to account for a maximum of 61% of total recharge based on comparison of diffuse recharge estimated from the unsaturated zone (0–43 mm yr^{-1}) and total recharge estimated from groundwater tracers (median 58 mm yr^{-1}) and water balance modeling (median 56 mm yr^{-1}). The results underscore the importance of lithologic controls on the distributions of both recharge rates and mechanisms.

Citation: Gates, J. B., G. V. Steele, P. Nasta, and J. Szilagyi (2014), Lithologic influences on groundwater recharge through incised glacial till from profile to regional scales: Evidence from glaciated Eastern Nebraska, *Water Resour. Res.*, *50*, doi:10.1002/2013WR014073.

1. Introduction

[2] Determination of groundwater recharge rates on spatial and temporal scales that are appropriate for groundwater resources management poses significant methodological challenges in many hydrogeologic settings [*de Vries and Simmers*, 2002; *Entekhabi and Moghaddam*, 2007; *Healy*, 2010; *Jyrkama and Sykes*, 2007; *Scanlon et al.*, 2002]. Although regional recharge predictions are accessible using a minimum of climate and soil-texture data [*Alcamo et al.*, 2003; *Dripps and Bradbury*, 2007; *Stanton et al.*, 2010], independent recharge assessments based on field measurements are necessary in order to develop sound conceptual models that can underpin quantitative model development [*Edmunds*, 2010; *Gates et al.*, 2008; *Manning and Caine*, 2007; *McMahon et al.*, 2011], to test or calibrate numerical models [*Döll and Fiedler*, 2007; *Ng et al.*, 2009; *Sanford*, 2002, 2011], and to provide historical recharge rates to identify trends that may stem from environmental changes [*Gates et al.*, 2011; *Gurdak et al.*, 2007; *Santoni et al.*, 2010; *Scanlon et al.*, 2007; *Tyler et al.*, 1996]. The challenges of recharge assessment are often most acute in areas where substantial spatial variability of recharge rates stem from sediment textural patterns, land use, topography, climatic gradients, or other factors.

[3] Groundwater recharge processes emerge from complex interactions between weather, sediment properties, and vegetation [*Feddes et al.*, 1988; *Healy*, 2010; *Nielsen et al.*, 1986; *Seyfried et al.*, 2005]. Drainage below the root zone occurs when water input rates from rainfall and other sources exceed rates of evapotranspiration and runoff generation for sufficiently long intervals for unsaturated flow to transmit moisture below the base of the root zone, at which point it becomes available to contribute to recharge after transmission through the unsaturated zone. As a result, changes in water inputs to the land surface, sediment hydraulic properties, and vegetation can all significantly affect recharge rates. A recent comparative study found

[1]Department of Earth and Atmospheric Sciences, University of Nebraska-Lincoln, Lincoln, Nebraska, USA.
[2]U.S. Geological Survey, Nebraska Water Science Center, Lincoln, Nebraska, USA.
[3]Department of Hydraulic and Water Resources Engineering, Budapest University of Technology and Economics, Budapest, Hungary.
[4]School of Natural Resources, University of Nebraska-Lincoln, Lincoln, Nebraska, USA.

Corresponding author: J. B. Gates, Department of Earth and Atmospheric Sciences, University of Nebraska-Lincoln, 217 Bessey Hall, Lincoln, NE 68588, USA. (jgates2@unl.edu)

0043-1397/14/10.1002/2013WR014073

that, on a global scale, variations in recharge rates are most strongly associated with water inputs and vegetation types [*Kim and Jackson*, 2012]. This statistical result dovetails with numerous case studies demonstrating strong impacts of land-use changes on recharge rates [*Cook et al*., 2001; *Gates et al*., 2011; *Scanlon et al*., 2007]. However, many studies on local to regional scales have shown strong sensitivity to sediment texture as well [e.g., *Cook et al*., 1992; *Heilweil and Solomon*, 2004; *Keese et al*., 2005; *Petheram et al*., 2002; *Rockhold et al*., 1995]. For example, the differences in recharge rates between the northern and southern portions of the US High Plains region have been primarily attributed to soil-texture differences [*Scanlon et al*., 2012]. Furthermore, studies of tillage impacts on agricultural water cycles have illustrated that soil-structure changes also can alter recharge rates on the plot scale [*O'Leary*, 1996; *Xu and Mermoud*, 2003].

[4] This study considers recharge to aquifers underlying incised glacial-till deposits. While several investigations have provided insights into unsaturated-flow processes through glacial till at the plot or profile scale [*Daniels et al*., 1991; *Espeby*, 1992; *Hendry*, 1983, 1988; *Hendry et al*., 2004; *Nilsson et al*., 2001], few have considered recharge through glacial till on the aquifer scale where landscape heterogeneities associated with geomorphic features such as river incision may have a significant impact [*Cuthbert et al*., 2010; *Gerber and Howard*, 1996, 2000]. A central challenge for improving conceptual models of such systems is, therefore, to better understand how landscape configurations affect the spatiotemporal variability in recharge. Conceptually, areas where clay-rich till deposits are locally absent because of river incising may provide the dominant source areas of recharge to underlying coarse-grained aquifers because hydraulic conductivities of clays are typically several orders of magnitude lower than those of coarse sediments. In river-incised glacial terrain, these eroded areas tend to primarily occur in lowlands along the flanks of river valleys [*Divine and Korus*, 2012]. Thus, a simplistic working hypothesis for areas with river-incised glacial-till deposits may be that diffuse recharge rates increase from higher topographic positions (clay-rich near-surface sediments) to lower topographic positions (silt or sand-rich sediments). On the other hand, several other factors affecting recharge rates including land use and preferential-flow processes may mitigate such a pattern. Incised glacial till therefore presents an opportune setting to assess whether spatial patterns in recharge rates mirror sediment textural distributions between fine and coarse-grained locations, or whether land use or other factors that affect soil-water budgets attenuate the pattern.

[5] Literature reviews on the topic of recharge assessment have consistently highlighted the value of applying multiple estimation methodologies in parallel in order to provide complementary information and to distance estimates from individual methodological biases [*Healy*, 2010; *Lerner et al*., 1990; *Scanlon et al*., 2002; *Simmers*, 1997]. While this practice unfortunately remains relatively uncommon, previous investigations have shown that there are significant advantages to combining methodologies based on saturated zone and unsaturated zone measurements [*Delin et al*., 2007; *Stadler et al*., 2010]. One advantage is that the two provide information on complementary spatial scales: monitoring of unsaturated zone moisture contents or matric potentials permits temporally explicit assessments of deep drainage and water redistribution from the surface to the water table, but only on the plot scale, whereas recharge estimates based on tracer measurements from groundwater samples can provide spatial and temporal integration, and hence can complement the unsaturated zone profile-based determinations by circumventing the need for a large number of monitoring sites. Moreover, groundwater tracer-based estimates integrate all recharge mechanisms, whereas unsaturated zone monitoring primarily reflects diffuse flow provided that the monitoring instrumentation is in locations that are not affected by focused or preferential flow.

[6] This study combines unsaturated zone monitoring with groundwater age-dating to provide information on recharge rates and variability through incised glacial till. The geologic configuration of the current study area in eastern Nebraska's glaciated landscape (Figure 1) provides an attractive natural laboratory to develop a conceptual framework of recharge patterns and temporal dynamics beneath incised glacial till. Specifically, it allows for a contrast of unsaturated zone flow conditions and groundwater residence times between uplands with intact glacial-till features and alluvial lowlands where till deposits have been eroded. The study's experimental design involves (1) tracking vertical and temporal soil-water dynamics at a combination of upland and lowland sites using unsaturated zone monitoring and environmental tracers, (2) assessing groundwater residence times at wells with varying distances from river valleys (where complete removal of till sediments has occurred) to uplands (where thick till sequences are present) using environmental tracers in groundwater, and (3) comparing local field results with regional gridded model-based recharge estimates in order to determine spatial representativeness of the field results. To our knowledge, it is the first investigation to compare relationships between recharge rates and sediment textural properties across nested profile, aquifer, and regional scales in a glaciated setting.

2. Study Area

2.1. Hydrogeologic Setting

[7] Principal aquifers for drinking water and irrigation in eastern Nebraska's glaciated region (eastern US Great Plains region; approximately 40–43°N and 95–98°W) are primarily associated with alluvial and glacial sand and gravel strata, many of which are overlain by clay-rich glacial till. These aquifers predominantly occur in modern or abandoned stream valleys or in elongated paleovalleys, although some sand and gravel-rich glacial deposits also result in isolated upland aquifers. Similar buried valley systems have been widely documented in glaciated landscapes in North America and elsewhere, and their importance to groundwater flow has been widely recognized [*Kehew and Boettger*, 1986; *Ritzi et al*., 2000]. The paleovalley aquifers in eastern Nebraska are among the most widely used groundwater resources in the region due to their significant size (in some cases $>$10 km wide and $>$100 km long) and favorable hydraulic properties. The paleovalleys are incised into underlying Cretaceous, Permian, and Pennsylvanian

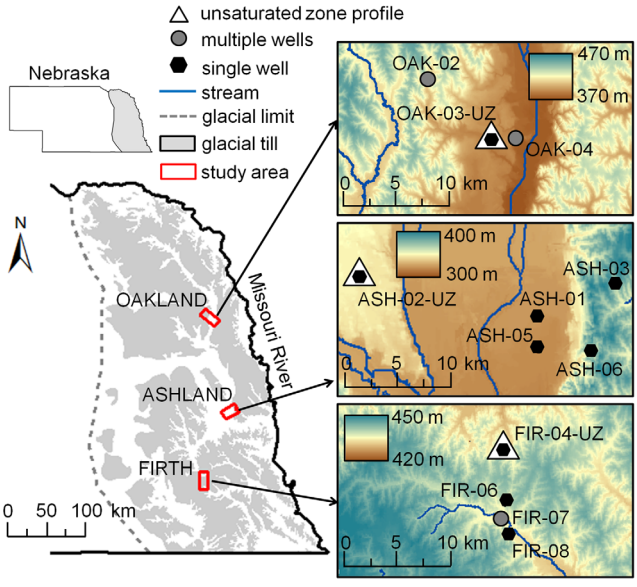

Figure 1. Study area maps and regional setting. White triangles denote unsaturated zone matric potential stations monitored continuously from 2008. Hexagons and circles represent well sites that were sampled in 2008 and 2009. Land surface elevation indicated from color ramp and given in meters above mean sea level. Gray area on the Nebraska state index map denotes the eastern Nebraska glaciated region. Glacial till delineations from *Divine et al.* [2009].

bedrock units along an overall east to west slope, and are thought to predate at least one advance of the Laurentide ice sheet prior to 640 ka. The paleovalleys have been the focus of recent characterization studies using airborne geophysics [*Abraham et al.*, 2012; *Korus et al.*, 2013]. However, the age of the coarse-grained paleovalley fills are not well constrained and may be preglacial, synglacial, or interglacial in origin. Tunnel valleys associated with subglacial drainage have been described in association with aquifers in many glacial settings [*Kehew et al.*, 2012, 2013; *Jørgensen and Sandersen*, 2006]. The possibility has been raised that some of the paleovalleys in the study area may be similar subglacial drainages that existed near the terminus of the Laurentide ice sheet during one of its retreats [*Korus et al.*, 2013], but current evidence of this origin remains equivocal.

[8] The succession of overlying unconsolidated sediments differs between upland areas and lowlands associated with the valleys of modern streams. Upland areas typically contain pre-Illinoian low-permeability glacial tills that were deposited during multiple glacial advances within the Pleistocene. Till thicknesses vary, but are generally thickest around topographic highs and can be up to 30 m thick. Till texture is also locally variable, but typically the tills are predominantly clay with interbedded sands and silts. Local sand bodies within the till units function as discontinuous upland perched aquifers in some cases. Across much of the study area, till units are overlain by loess deposits that range from ~14,000 (Peoria Loess) to ~160,000 (Loveland Loess) years in age. Local combined thicknesses of loess units can be up to ~30 m in some areas. The upland landscape is dissected by stream valleys in which till and loess layers have been eroded by alluvial processes and are no longer present (although some older stream terraces at the margins of these valleys may still be mantled by Peoria Loess). Alluvial fill deposits within the stream valleys overlie bedrock and are also used as aquifers in some locations.

[9] This investigation is organized around three study areas, referred to below as the Oakland (OAK), Ashland (ASH), and Firth (FIR) study areas, the positions of which were selected to be broadly representative of the region's hydrogeologic conditions (Figure 1). The Oakland study area is located within an area of stream-dissected glacial hills where rolling topography and a stream valley has been eroded out of thick glacial deposits overlain by loess units [*Abraham et al.*, 2012; *Gosselin et al.*, 1996; *Nasta and Gates*, 2013]. The Ashland study area is within an area of loess-capped till that has been dissected by a large alluvial system (the Platte River). Alluvial terrace deposits occupy some lower to intermediate topographic positions in the Ashland area. The Firth study area coincides with glacial till that overlies a large paleovalley [*Divine et al.*, 2009]. Unsaturated zone thicknesses range from essentially zero in lowland areas adjacent to surface water up to ~60 m in uplands. The Cretaceous Dakota Formation that underlies the Oakland study area and outcrops near the Ashland study area [*Divine et al.*, 2009] hosts groundwater of elevated salinity that is a source of salinization to surface waters in the region [*Gosselin et al.*, 2003; *Harvey et al.*, 2007]. Bedrock underlying the Ashland and Firth study areas is predominantly Pennsylvanian and Lower Permian limestone and shale units [*Divine et al.*, 2009].

[10] Piezometric gradients suggest that groundwater flow is generally from upland areas toward lowlands where groundwater discharges to streams including Logan Creek (Oakland study area), the Platte River (Ashland study area), and Big Nemaha River (Firth study area), although locally heterogeneous groundwater flow conditions likely exist in some upland areas in association with hilly topography and textural heterogeneity. Lowland groundwater flow in the Ashland study area generally parallels the Platte River. Remnants of the Pleistocene Platte River valley (Todd Valley) intersect with the modern Platte River valley near the western edge of the study area, and provide significant volumes of water to the Platte River and adjacent groundwater [*Steele*, 2002].

2.2. Land Use and Climate

[11] Land use is primarily a combination of irrigated and rainfed row crops (typically corn/soybean rotation), rangeland (pasture) and prairie grassland. Land use at the unsaturated monitoring sites includes rainfed row crops (OAK-03-UZ), irrigated row crops (ASH-02-UZ), and (nonirrigated) prairie grassland (FIR-04-UZ; section 3.1). Average annual precipitation from 1953 to 2008 in the Oakland, Ashland, and Firth study areas were 718, 768, and 822 mm, respectively (http://www.ncdc.noaa.gov/; last accessed 4 December 2012; Table 1). Daily mean temperatures at the three study areas range from approximately −1 to −3°C in the winter and 22–24°C in the summer (http://www.hprcc.unl.edu/data/historical/index.php; last accessed 4 December 2012; station records 1985–2012 for Oakland, 1982–

2012 for Ashland and 2009–2012 for Firth). Precipitation occurs primarily as convective storms during spring and summer, and a combination of convective and stratiform rainfall and snowfall during winter and fall. Despite similar long-term climatic normals, differences in P and ET_p were apparent among the sites during the 2009–2012 monitoring period (Table 1). Precipitation at OAK-03-UZ was the highest of the three sites, especially during the 2012 drought year, whereas potential evapotranspiration values were highest at FIR-04-UZ, implying that rainfall deficits generally increased from north to south.

3. Methods

3.1. Overview of Experimental Design

[12] Groundwater recharge estimates were developed on three nested spatial scales: vertical profile (plot scale), aquifer scale, and regional scale. Profile scale: Unsaturated zone profile matric potential monitoring was undertaken at three sites in order to provide estimates of diffuse recharge and to contrast temporal and vertical dynamics of deep drainage through lowland (OAK-03-UZ in the Oakland study area) versus upland unsaturated zones (ASH-02-UZ in the Ashland study area and FIR-04-UZ in the Firth study area; Figure 1; section 3.2.1). A second upland site was desirable because of the variety of land uses in the upland portions of the study area. The lowland profile (OAK-03-UZ) is within alluvial sediments and as a result has the most vertically uniform texture (average 3% sand, 62% silt, and 34% clay; Figure 2). Matric potentials from OAK-03-UZ have been previously presented in the context of 2012 drought impacts [*Nasta and Gates*, 2013]. ASH-02-UZ has high clay and silt percentages in the top 4 m (average 60% silt and 32% clay in 0–4 m), and then rapidly coarsens with depth to a maximum of 98% sand at 11.4 m depth. FIR-04-UZ ranges from 26 to 48% clay, with highest clay percentages near the soil surface and below 6 m. Unsaturated zone tracers (^3H and Cl^-) provide two additional deep drainage estimates for FIR-04-UZ (section 3.2.2). Aquifer scale: Estimates of total recharge (diffuse plus nondiffuse) were developed from groundwater tracer distributions (CFC-12 and SF_6) in locations ranging from river valleys to uplands in order to facilitate comparison across topographic gradients (section 3.3). Each of three study areas included five wells from which tracer samples were collected; three of the wells were colocated with an unsaturated zone monitoring station (OAK-03-15, ASH-02-59, FIR-04-40). Additional parameters measured at each well included tritium, temperature, selected redox indicators (O_2, NO_3^-, Fe^{2+}, Mn^{2+}, SO_4^{2-} and CH_4), N_2, and Ar, in order to support CFC-12 and SF_6 interpretation. Regional scale: The three study areas were selected to broadly reflect the range of hydrogeologic conditions within the glaciated region bounded by the westernmost extent of glaciation in Nebraska and the Missouri River, but they represent <1% of this total land area (Figure 1). In order to better place field results in the context of regional recharge, results from a remote sensing-assisted water balance model [*Szilagyi and Jozsa*, 2012] were reanalyzed as a function of unsaturated zone thickness across the region (45,000 km^2 with 1 km^2 resolution for 2000–2009; section 3.4) and compared with the field results from the saturated and unsaturated zones. Details of each method are presented below.

3.2. Profile-Scale Methods

3.2.1. Unsaturated Zone Physical Methods

[13] Matric potentials in the unsaturated zone were monitored using heat dissipation sensors (Model 229, Campbell Scientific, Logan UT; background on sensor use is provided by [*Flint et al*., 2002] and [*Brock et al*., 1995]; locations are shown in Figure 1 and sensor positions are shown in Figure 2). Monitoring records were available from 2008 to 2012 for OAK-03-UZ and FIR-04-UZ. Only 2008–2010 is available for ASH-02-UZ because of electronic failure in 2011. All profiles include sensors both within and below the root zone in order to provide information about transient moisture fluxes across the base of the root zone (~1.5 m at OAK-03-UZ and ASH-02-UZ; ~0.5 m at FIR-04-UZ). The sensor profiles reach the capillary fringe at OAK-03-UZ (regional water table) and FIR-04-UZ (perched upland water table); the bottommost ASH-02-UZ sensor is 2 m above the regional water table. Sensors were individually calibrated using laboratory pressure chambers and installed encased in silica flour to ensure continuous hydraulic contact with surrounding sediments. The profiles were capped to prevent artificial preferential flow around backfilled sediments or sensor cables. Sensor heat pulses were triggered every four hours to provide quasi-continuous matric potential time series, which were recorded with solar-powered data loggers. Core sediments removed during sensor installation were analyzed for texture, saturated hydraulic conductivity (K_s), saturated water content (θ_s), and soil hydraulic parameters (θ_r, α, and n; [*van Genuchten*, 1980]) using standard laboratory methods (U.S. Geol. Surv. California Water Science Center Geotechnical Laboratory; ASTM procedures C136 and D5084; [*Klute*, 1986]; Table 2).

[14] Deep drainage rates were estimated from matric potentials and unsaturated hydraulic conductivity measurements using the Buckingham-Darcy equation (Table 2). A unit gradient simplification was employed for the calculation for ASH-02-UZ. Drainage rate uncertainties were estimated stochastically taking into account error distributions in the matric potential measurements and unsaturated hydraulic conductivities. The parameter values of the unsaturated hydraulic conductivity functions and heat dissipation sensor calibration functions were estimated through an optimization routine included in the RETC model code [*van Genuchten et al*., 1991] assuming that all errors were

Table 1. Annual Precipitation and Potential Evapotranspiration for Matric Potential Monitoring Sites

	OAK-03-UZ				ASH-02-UZ		FIR-04-UZ			
	2009	2010	2011	2012	2009	2010	2009	2010	2011	2012
P (mm)	439	654	803	465	562	737	583	529	572	246
ET_p (mm)	746	677	711	723	637	713	765	824	794	1027

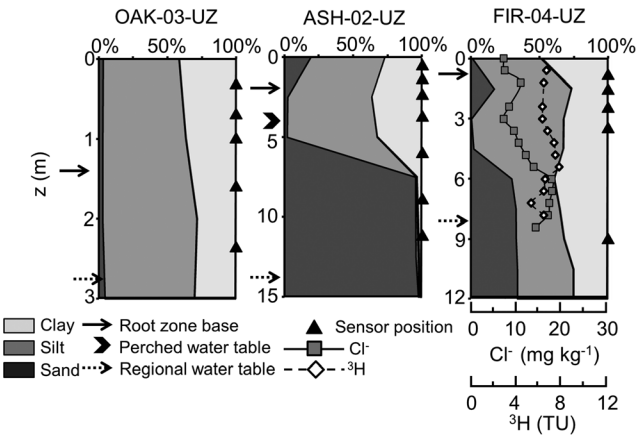

Figure 2. Characterization of unsaturated zone physical and chemical properties based on sediment cores collected during sensor installation. Positions of heat dissipation sensors and nominal positions of water tables and root zone bases also shown.

normally distributed (Table 2). The uncertainty estimate was then obtained by generating 10,000 replicates of the deep drainage flux calculation with hydraulic conductivity functions and heat dissipation sensor calibration function parameters drawn randomly from their respective error distributions. The reported uncertainty is equal to the difference between minimum and maximum replicates.

3.2.2. Unsaturated Zone Chemical Methods

[15] Pore water was analyzed for Cl^- and ^3H in the sediment profile collected from FIR-04-UZ monitoring site (Figure 2). Pore water for ^3H measurement was extracted with vacuum distillation at about 90°C and analyzed with liquid scintillation counting (USGS Tritium Laboratory, Menlo Park, CA). Analytical precision for individual samples ranged from ±0.5 to ±4.0 TU. Pore waters analyzed for Cl^- were extracted with deionized water elutriation and analyzed with ion chromatography. Unsaturated zone Cl^- and ^3H mass balance methods have been previously described in detail [*Allison and Hughes*, 1978; *Cook et al*., 1994] and are briefly summarized here. Tracer masses above an intermediate position in the unsaturated zone (below the root zone and above the capillary fringe) are assumed to be attributable to atmospheric inputs only (no terrestrial sources). For Cl^-,

$$q = C_p P / C_R(z_m) \tag{1}$$

where q (L T^{-1}) is the apparent recharge rate above maximum profile depth z_m (L), C_p (M L^{-3}) is the mean Cl^- concentration in precipitation and $C_R(z_m)$ (M L^{-3}) is the average measured Cl^- concentration of pore waters above depth z_m.

^3H mass balance is similar but corrects for ^3H decay and interannual variations in drainage [*Cook et al*., 1994]:

$$q = \frac{\int_0^{z_m} \theta(z) C(z) dz}{\sum_{i=2}^{i=2} \omega_i C_i e^{-t\lambda}} \tag{2}$$

where t (T) is time, C_i (M L^{-3}) is the present ^3H concentration of rainfall i years before present, $\theta(z)$ (L^3 L^{-3}) is volumetric moisture content at depth z, λ (T^{-1}) is the decay coefficient, and ω_i is a weighting function for annual rainfall contributions to profile soil-water equal to the ratio of rainfall in year i to the long-term average.

[16] Mass inputs of Cl^- and ^3H were assumed to be from atmospheric sources only. Atmospheric Cl^- wet deposition was specified using the long-term mean annual value (0.73 kg ha^{-1}) from the National Atmospheric Deposition Program station in Mead NE (1978–2010; 75 km northeast of the Firth site). Dry deposition has not been measured in the study area; therefore, it was assumed that dry deposition occurred at an equal rate to wet deposition (i.e., total wet plus dry deposition of Cl^- was estimated by multiplying the wet deposition value by two). This assumed rate of dry deposition has been used previously in recharge studies in the Great Plains in the absence of robust dry deposition data for Cl^- [*Scanlon et al*., 2007]. Some authors have also used model-derived dry fallout estimates from the USEPA Clean Air Status and Trends Network (CASTNET), which are generally lower than wet deposition in this region. The ^3H concentration in precipitation was estimated using historical records from Lincoln NE (1962–1986; 30 km north of the Firth site; Robert Michel, U.S. Geological Survey, personal communication, 2004); and Mead NE (Global Network of Isotopes in Precipitation; International Atomic Energy Agency; http://www-naweb.iaea.org/napc/ih/IHS_resources_gnip.html; last accessed 4 December 2012). For periods of missing data, the ^3H record in precipitation was reconstructed using correlation coefficients from periods of overlap with the Ottawa record [*Michel*, 2005].

[17] Cl^- and ^3H mass balance recharge rate estimates are only reported for FIR-04-UZ because, as a non-cultivated grassland site with a relatively deep water table, it is the only one of the three unsaturated zone profile sites with well-constrained input functions of Cl^- and ^3H to the profile. The Oakland profile is affected by capillary rise from the water table, and the Ashland profile receives water from groundwater irrigation with concentrations of Cl^- and ^3H that are likely to be temporally variable. In both cases, developing reliable Cl^- and ^3H input functions to the profile is impossible with available data. Uncertainties in chloride-based recharge estimates have been previously addressed in detail [*Scanlon*, 2000]. At this location, dry

Table 2. Hydraulic Parameters Measured From Field Cores Used to Estimate Drainage Rates With the Buckingham-Darcy Equation

Site	Depth (m)	θ_r (cm^3)	θ_s (cm^3)	α (mm^{-1})	n	K_s (mm d^{-1})
OAK-03-UZ	2.3	0.085 ± 0.0066	0.511	0.0013 ± 0.00038	1.09 ± 0.0081	8.45 ± 0.407
ASH-02-UZ	6.0	0.008	0.349	0.0020	2.84	2720.68
FIR-04-UZ	3.0	0.081 ± 0.0027	0.515	0.00093 ± 0.000053	1.28 ± 0.013	2732.5 ± 10.6

deposition is likely to be the largest source of uncertainty in Cl^- mass balance applications (errors in atmospheric deposition estimates scale linearly to errors in recharge). For recharge estimate intercomparison purposes, a nominal 50% uncertainty range for the FIR-04-UZ chloride-based recharge estimate is assigned based on the poorly constrained range of dry deposition rates. An uncertainty range of 25% is assigned for the FIR-04-UZ ^3H mass balance recharge estimate based on previous approximations [*Cook et al*., 1994; *Sukhija and Shah*, 1976].

3.3. Aquifer-Scale Methods

3.3.1. Groundwater Tracers

[18] Wells were installed with a combination of percussion and rotary drilling depending on depth and lithology. Concentrations of $CFCl_3$ (CFC–11), CF_2Cl_2 (CFC–12), $C_2F_3Cl_3$ (CFC–113) and SF_6 were measured for groundwater residence-time estimation. Of the three CFCs, only CFC-12 was used quantitatively because it was the least affected by degradation under reducing conditions, which were found to be prevalent. Samples for analysis of dissolved gases were collected from purged wells using the submerged bottle methods described by *Busenberg et al*. [2006] and analyzed using electron-capture gas chromatography (USGS Chlorofluorocarbon Laboratory, Reston VA; http://water.usgs.gov/lab/dissolved-gas/sampling/). Water samples for ion analyses were collected using a dedicated submersible pump using low-flow purging. Teflon bailers were used on occasions when wells had water yields that were insufficient for collection using a submersible pump. Samples were chilled to 4°C, acidified to $pH < 2$ (cation aliquots only), and analyzed using standard methods (Midwest Laboratories, Omaha NE; analytical procedures listed at https://www.midwestlabs.com; last accessed 24 August 2012). Field water temperature and O_2 were measured with a portable water quality meter at the time of sampling.

3.3.2. Residence Time Estimation

[19] CFC-12 and SF_6 tracer age calculations are contingent upon historical atmospheric input functions, water temperature and atmospheric pressure during recharge, correction for nonequilibrium gas sources (excess air), and mixing [*Cook and Böhlke*, 2000]. Monotonically increasing atmospheric concentrations from the 1960s to present in North America permits unique air equilibrium SF_6 values after about 1970 to be calculated for a given recharge year, equilibration temperature, and atmospheric pressure using Henry's Law. Stabilization of CFC concentrations in air during the 1990s and subsequent decline in the 2000s makes CFC-based age discrimination difficult for recently recharged waters. Historical atmospheric concentrations from the Niwot Ridge CO record are used here and should be representative for the study area [*Busenberg et al*., 2006; *Darling et al*., 2012], although local CFC-12 contamination prevents reliable dating for a subset of shallow groundwater samples. Recharge elevations were assumed equal to sample elevations, which is an adequate estimate given the study area's limited topographic relief (~60 m). Atmospheric pressures were determined from recharge elevation using the atmospheric lapse rate. Recharge temperatures were estimated by statistical fit to a closed-system equilibration model (CE model) [*Aeschbach-Hertig et al*., 2000] using measured Ar and N_2 concentrations. CE model results were also used to correct measured tracer concentrations for excess air.

[20] Groundwater residence times were estimated using CFC-12/SF_6 tracer mixing plot positions where possible. Eight of 15 samples fell within the CFC-12/SF_6 mixing space, and the sample plot positions for these samples were used to determine the appropriate age model. For the seven of 15 samples that had insufficient tracer data to assess mixing status (due to either contaminated or degraded levels of CFC-12), a piston flow age model was assumed, and age was based solely on SF_6. Age model parameter optimizations to gas concentration data were performed using the TracerLPM best-fit algorithm [*Jurgens et al*., 2012]. Uncertainty in residence times may derive from a potentially large number of factors including errors in recharge temperature and elevation estimation, excess air, and nonconservative tracer behavior in the subsurface [*Hinsby et al*., 2007; *Massoudieh et al*., 2012; *Sebol et al*., 2007]. Failure to correctly take into account mixing processes and diffusive transport can also severely bias age estimates [*Weissman et al*., 2002; *Troldborg et al*., 2008]. In this study, age uncertainties were estimated using Monte-Carlo methods taking into account analytical errors in CFC-12, SF_6, N_2, and Ar (N_2 and Ar uncertainties affect ages through the recharge temperature and excess air estimates.) All errors were assumed to be normally distributed and 1σ (standard deviation) age ranges from 1,000 iterations per sample are reported; age ranges for samples FIR-07-63 and FIR-04-40 additionally take into account potential ambiguity in mixing model assignment.

3.3.3. Recharge Rate Estimation From Residence Times

[21] Previous recharge rate estimations from groundwater ages of samples collected near the water table have commonly assumed a linear age gradient between the water table and the sample depth [*Cook and Böhlke*, 2000; *McMahon et al*., 2011]:

$$q = \frac{z_g \Phi}{t_R} \tag{3}$$

where z_g (L) is annual average depth below the water table of the midpoint of the well screen, Φ is porosity ($L^3\ L^{-3}$), and t_R (T) is the residence time. For recharge estimation from groundwater ages in deeper wells, some authors have assumed a logarithmic age-depth relationship:

$$q = \frac{\phi Z}{t_R} \ln\left(\frac{Z}{Z - z_g}\right) \tag{4}$$

where Z (L) is saturated thickness of the aquifer [*Vogel*, 1967]. Equation (4) is based on several simplifying assumptions including uniformly distributed recharge and hydraulic properties [*Böhlke*, 2002]. Equations (3) and (4) are used to estimate recharge from the subset of samples in this study that lack evidence of mixing from CFC-12 and SF_6. However, approximately half of all samples have tracer plot positions that suggest mixtures of young water and old water from immobile water and/or upward leakage from underlying units. To estimate recharge rates from these samples, it

was assumed that mixing ratios are simple binary mixtures between young and old (i.e., tracer-free) water, and that only the young water fraction derives from meteoric recharge. As a way to account for the tracer dilution from old water, the apparent age of the young water fraction is assigned to t_R, and the age gradient is adjusted downward to account for old water contributions to the sample:

$$q = \frac{z_g \phi f}{t_R} \tag{5}$$

$$q = \frac{Z \Phi f}{t_R} \ln\left(\frac{Z}{Z - z_g}\right) \tag{6}$$

where f is the young water component mixing fraction. The magnitude of this correction is proportional to the estimated young fraction percentage. It is emphasized that equations (5) and (6) are presented only as a means to estimate recharge rates from individual groundwater samples that are binary mixtures of waters with differing ages, and in the absence of vertical or temporal tracer gradients. All limitations to equations (3) and (4) also apply to equations (5) and (6), in addition to the assumption that the tracer distributions represent simple binary mixtures, which is not possible to independently confirm with available data. Reported uncertainty ranges for the recharge estimate take into account the 1σ residence time ranges (section 3.3.1) and the range of values obtained using both equations (5) and (6).

3.4. Regional-Scale Methods

3.4.1. Water-Balance Model

[22] Regional distributions of recharge rates are assessed through a reanalysis of earlier recharge mapping results [*Szilagyi and Jozsa*, 2012], where monthly actual evapotranspiration rates for 2000 to 2009 were estimated with 1 km^2 resolution using linear transformations of daytime surface temperatures using the Priestley-Taylor equation and the complementary relationship of evaporation [*Szilagyi and Jozsa*, 2012]. The difference between monthly gridded precipitation and actual evapotranspiration was assumed equal to the sum of recharge and runoff. Recharge was then partitioned from runoff using a power-function transformation of the DRASTIC model code value [*Aller et al*., 1987*; Rundquist et al*., 1991]. The approach has been shown to agree well with field recharge estimates in previous investigations [*Szilagyi et al*., 2011]. In this study, 1 km^2 gridded recharge estimates for the study area were aggregated as a function of unsaturated zone thickness. Unsaturated zone thickness is used as a proxy indicator of regional till cover given that detailed till lithology is only available for smaller subareas within the study region. Unsaturated zone thickness was calculated from the difference in surface elevation and water table elevation GIS raster coverages (http://snr.unl.edu/data/geographygis/NebrGISdata.asp).

4. Results and Discussion

4.1. Profile-Scale Recharge

4.1.1. Unsaturated-Zone Dynamics in Lowland and Upland Profiles

[23] The matric potential time series at OAK-03-UZ (Figure 3) represents an example of lowland, till-absent conditions. The matric potential time series at ASH-02-UZ and FIR-04-UZ represent uplands with intact glacial till sediments (Figures 4 and 5). The top two sensors at OAK-03-UZ (0.30 and 0.61 m sensors) display seasonal temporal dynamics in which minimum (dry range) matric potentials tend to follow periods of peak ET_p, which occur during the summer growing season. However, intermittent wetting and drying trends are apparent throughout the monitoring period associated with individual rainfall events. OAK-03-UZ sensors at 1.52 m and 2.44 m show near saturated conditions throughout the majority of the monitoring period due to the site's shallow water table (water table position of approximately 3 m below surface at time of installation). Matric potential variability in ASH-02-UZ is subdued at all depths because of the combination of irrigation applications to the surface (center pivot sprinkler) and sediment saturation at ~4 m (moisture contents from core samples collected during sensor installation at ASH-02-UZ in May 2008 show saturated conditions at 3.8 m below surface). The saturated layer coincides with relatively high clay contents indicative of glacial till (up to 36% clay; Figure 2). Below the perched layer, the sand-rich sequence from 9 to 12 m in ASH-02-UZ (which is likely to be associated with glacial deposition given its significant distance from the area's alluvial sediments) had low matric potentials throughout the monitoring period (range $-1.6 < \psi < -1.2$ bars), indicating that the clay-rich till above 4 m functions as a barrier to drainage. Wetting and drying trends in the other upland site (FIR-04-UZ) for sensors below the root zone (2.4 and 3.3 m) suggest that intermittent drainage below the root zone takes place at this site also. Matric potential variations at FIR-04-UZ are less obviously seasonal than OAK-03-UZ, and this may be associated with the fact that vegetation at FIR-04-UZ is perennial, in contrast to the seasonal cropping pattern at OAK-03-UZ.

4.1.2. Unsaturated Zone Profile-Based Diffuse Recharge Estimates

4.1.2.1. Lowland Rainfed

[24] Recharge rates to the paleovalley aquifer at OAK-03-UZ were estimated for 2009–2012 using matric potentials from the 1.5 m and 2.4 m sensors and the $K(\psi)$ measurement at 2.3 m. Annual rates varied between 36 mm in 2011 and 10 mm in 2012. The arithmetic average for the 4 year period was 21 mm yr^{-1} for OAK-03-UZ.

4.1.2.2. Upland Irrigated

[25] Recharge rates to the paleovalley aquifer at ASH-02-UZ were estimated for 2009–2012 using matric potentials from the 12 m sensor in the sand stratum below the saturated clay-rich layer and the $K(\psi)$ measurement at 6.0 m, which was the nearest available $K(\psi)$ measurement in the sand layer. Based on these values, drainage beneath the clay-rich till layer was essentially zero for 2009–2010 (10^{-4} mm yr^{-1}). This calculation is consistent with the inference from matric potential time series that the till layer provides an effective barrier to deep drainage at this site. Estimation of recharge rates to the overlying perched zone was not attempted at this location (see section 3.1).

4.1.2.3. Upland Grassland

[26] Recharge rates to the perched aquifer at FIR-04-UZ were estimated for 2009–2012 using matric potentials from the 2.4 m and 3.3 m sensors and the $K(\psi)$ measurement at 3.0 m. Annual recharge rates ranged between 4 mm in

2009 and 12 mm in 2011. The arithmetic average for the 4 year period was 9 mm yr^{-1}. Long-term average recharge rates for FIR-04-UZ were also estimated using Cl^- mass balance and ^3H mass balance. Cl^- mass balance yielded a recharge rate of 5 ± 3 mm yr^{-1} based on estimated annual atmospheric fallout rate of 1.45 and 648 kg ha^{-1} measured in the profile. ^3H mass balance yielded 34 ± 9 mm yr^{-1} based on an estimated 552 TU m deposition and 23.3 TU m measured in the profile.

4.1.3. Timing of Deep Drainage Generation

[27] The sensor pair used for the Buckingham-Darcy calculation for OAK-03-UZ is immediately below the base of the root zone (1.5 and 2.4 m), and therefore, is well suited to illustrate the temporal patterns in generation of subroot zone drainage at the site (Figure 6). Between 1 January and 8 September of 2009 there was a fairly constant drainage rate of 0.10 mm/d (i.e., ~26 mm/yr). In 2009 near the end of the summer growing season, soil water depletion resulted in a period of upward water potential gradients between September 2009 and January 2010 (discharge of about 10 mm during this period). Between 18 March 2010 and 23 April 2012, water potential gradients were consistently downward (average recharge rate for this period was 35 mm/yr). The absence of a matric potential gradient reversal in 2010 and 2011 is likely attributable to frequent rainfall events distributed during the growing season, which was sufficient to fulfill crop water demand. Another period of upward water potential gradients began during summer 2012 during a period of severe regional drought and persisted through the end of the record in December 2012 (8 mm discharge estimated between June and December 2012).

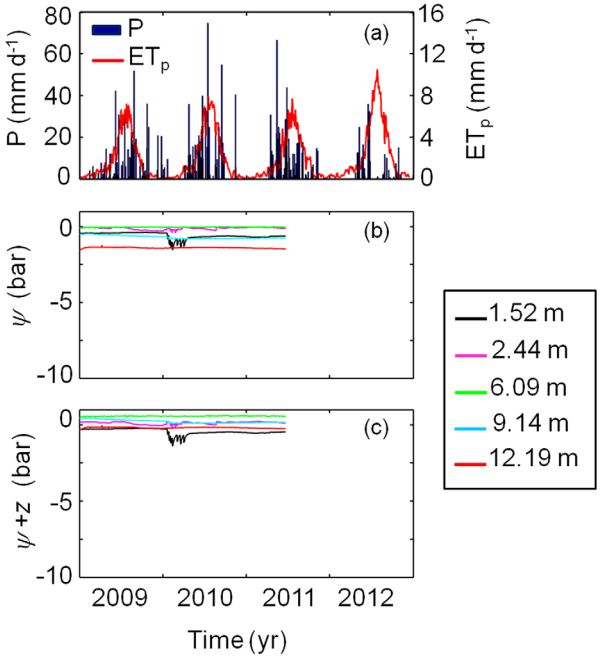

Figure 4. Time series data for ASH-02-UZ including (a) precipitation and potential evapotranspiration, (b) matric potentials, and (c) total potentials.

4.2. Aquifer-Scale Recharge

4.2.1. Temperature and Excess Air Corrections

[28] Results for CFC-12 and SF_6 listed on Table 3 are given as both raw concentrations and atmospheric mixing ratios corrected for excess air amounts estimated with the

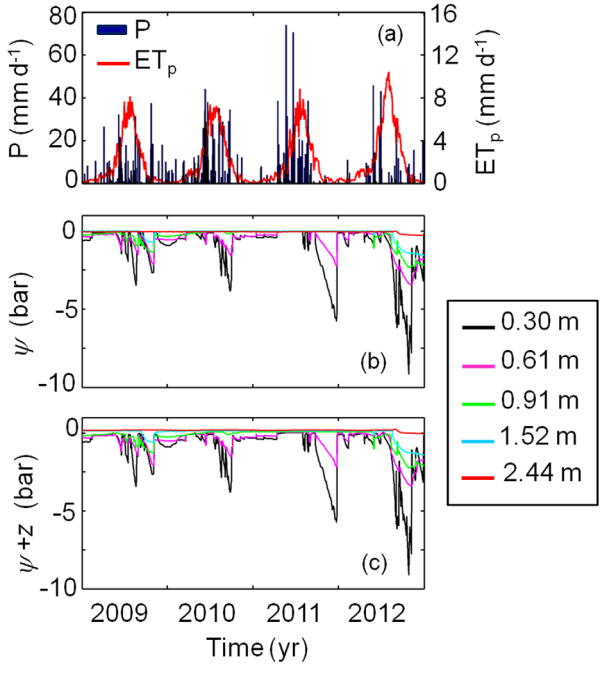

Figure 3. Time series data for OAK-03-UZ including (a) precipitation and potential evapotranspiration, (b) matric potentials, and (c) total potentials.

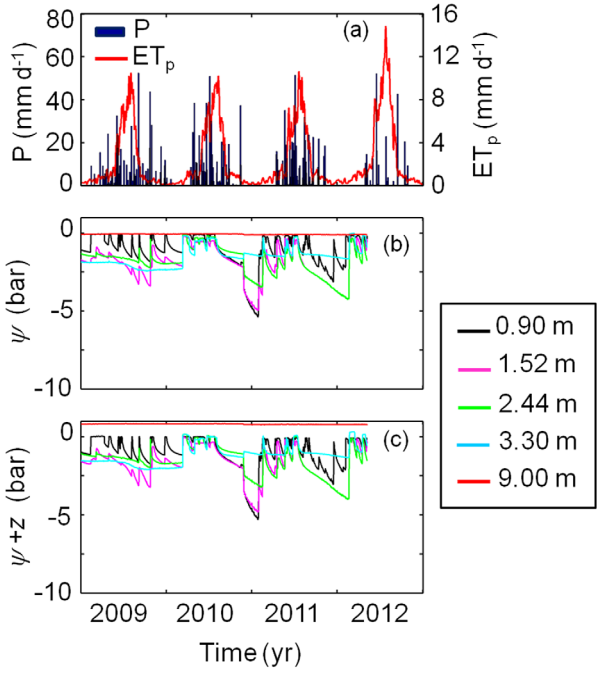

Figure 5. Time series data for FIR-04-UZ including (a) precipitation and potential evapotranspiration, (b) matric potentials, and (c) total potentials.

CE model fit to N_2/Ar data. Excess air amounts were all <8 $cm^3\ kg^{-1}$ and generally <4 $cm^3\ kg^{-1}$ (Table 3); these excess-air concentration ranges are likely attributable to air entrapped during water-table fluctuations [*Wilson and McNeill*, 1997]. The highest excess air values in the data set were found in samples from the Oakland study area. Wells within this study area are mostly completed within a paleovalley aquifer unit that experiences significant pumping from irrigators and a municipal well field. The elevated excess-air concentrations in this area relative to the other two may therefore be associated with larger water-table fluctuations. Recharge temperatures estimated with the CE model ranged from 4 to 14°C and were lower than sample temperatures with the exception of one well (ASH-05–15), suggesting that heating in the subsurface took place prior to sampling in most cases (mean sample temperature 3.8°C above its corresponding apparent recharge temperature; Figure 7). Differences between apparent recharge temperatures and mean annual air temperatures over each station's monitoring period ranged from −5.1 to +4.9°C, with an average difference of −0.9°C for all samples; Figure 7).

4.2.2. Groundwater Ages and Mixing

[29] Mean tracer ages are strongly dependent upon mixing processes during groundwater flow or within the sampling well [*Plummer*, 2005]. In complex glacial terrain, selection of appropriate mixing models based on flow system conceptualization is difficult because of the likelihood of localized confinement and heterogeneous flow systems. Figure 8 shows CFC-12 and SF_6 concentrations relative to a piston flow model as well as hypothetical binary mixing ratios [*Cook and Böhlke*, 2000; *Maloszewski and Zuber*, 1996]. Eight of 15 samples fall within the CFC-12/SF_6 mixing space bounded by the piston flow model and a binary mixing model with a young fraction age of 2 years (Figure 8). Most samples that plot within the CFC-12/SF_6 mixing space appear to be mixtures of different water ages, based on their plot positions to the left of the piston flow line. The two samples from intermediate topographic positions within the Firth area (FIR-04-40 and FIR-07-63) plot near the intersection of the piston flow model and binary mixing lines of 10 and 20 years. In those cases, it is difficult to distinguish between piston flow and binary mixing based on available data; hence, the uncertainty ranges reported for those samples take into account both of the corresponding age estimates. Groundwater from FIR-06-40 appears to be recently recharged based on its position near the modern confluence of the tracer curves.

[30] Residence time estimates ranged from ∼0 to 25 years for samples evaluated using the piston flow model, and 2 to 20 years for young water fractions of samples evaluated using the binary mixing model (Table 3). ^3H activities ranged from <0.1 to 16.6 TU (Table 3). Thirteen of 15 samples had detectable ^3H, which is broadly consistent with the ages developed from CFCs and SF_6. Three samples plotting to the left of the mixing space have likely been affected by CFC-12 degradation under reducing conditions based on redox indicators (Table 4 and Figure 8). OAK-04-89 and ASH-05-15 had trace methane present, as well as excess N_2 and low NO_3^-, which are indicative of denitrification. OAK-02-172 had no detectable methane but had low O_2 and NO_3^- and detectable Fe^{2+} and Mn^{2+}. Although ASH-03-108 had a relatively low CFC-12 concentration (43 pptv) and plots to the left of the CFC-12/SF_6 mixing space, there is no other indication of CFC-12 degradation; this groundwater was oxidizing based on all available redox indicators. Given that the ASH-03–108 sample also had $^3H < 0.1$ TU, it is possible that it has an age >50 years and had slight SF_6 and/or CFC-12 contamination during sampling. SF_6 contamination of a sample with age near the upper end of the CFC-12 dating range (∼1960s recharge) also could have caused the vertical offset of this sample from the mixing envelope on the tracer plot in Figure 8. Two Ashland samples that plot to the right of the mixing envelope were likely affected by CFC-12 contamination (CFC-12 in ASH-06-59 far exceeds equilibrium concentrations with modern atmosphere; CFC-12 in ASH-01-50 is below equilibrium with modern atmosphere but is too high to be consistent with any mixing model at observed SF_6 concentrations). All sampled wells had SF_6 concentrations that were at or below saturation with respect to water in equilibrium with modern atmosphere at field temperatures and pressures after correcting for excess air. (FIR-06-40 is the only sample with SF_6 at saturation with respect to modern atmospheric concentrations.) Some contamination with naturally produced SF_6 has been previously reported for groundwater samples from glacial tills [*Busenberg et al*., 2001] and in the High Plains aquifer ∼100 km west of the study area [*Eberts et al*., 2012], but the present data set contains no clear SF_6 contamination signature.

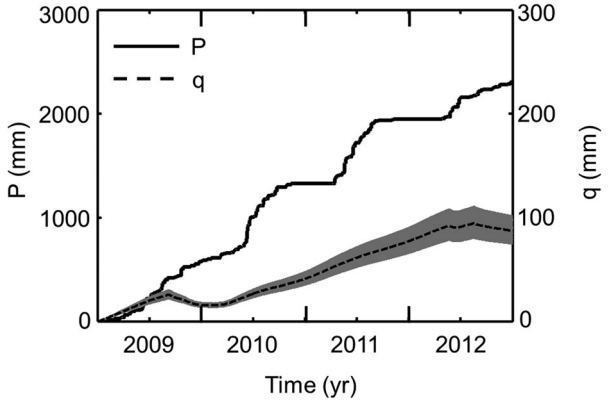

Figure 6. Cumulative recharge values (black lines) with associated uncertainty bands (gray lines) at OAK-03-UZ based on measured matric potentials and the Buckingham-Darcy equation. Cumulative rainfall at OAK-03-UZ also shown for reference.

4.2.3. Tracer-Based Recharge Estimates

[31] While CFC-12 and SF_6 concentrations at the water table generally reflect equilibrium with atmospheric concentrations in settings with shallow water tables, significant vapor phase transit times through thick and/or low-porosity unsaturated zones can cause time lags between atmospheric input functions and gas concentrations near the water table. Gas transport modeling suggests that, in general, unsaturated-zone time lags tend to become significant for groundwater age estimations when water tables exceed ∼10 m depth [*Cook and Solomon*, 1995]. However, lag times are sensitive to porosity, moisture content and tortuosity [*Cook and Solomon*, 1995; *Engesgaard et al*., 2004], and field data on unsaturated-zone gas transport lag times within undulating

Table 3. Tracer Results and Model Parameter Values for Groundwater Samples[a]

	N2 (mmol/kg)	Ar (mmol/kg)	CFC-12 (pmol/kg)	SF6 (fmol/kg)	Excess Air (ccSTP/kg)	Recharge Temperature (°C)	SF6 (pptv)	CFC-12 (pptv)	Φ(−)	Z (m)	z_g (m)	f(−)	t_R (yr)	Age Model	^{3}H (TU)
OAK-02–34	7.13×10^{-1} (±1%)	1.77×10^{-2} (±1%)	2.06 (±0.1%)	1.88 (±3%)	2.6 (2.1–3.1)	9.3 (8.5–10.2)	3.77 (3.49–4.08)	379.1 (361.9–403.7)	0.20	2.5	1.7	0.66 (0.66-0.74)	3.9 (2.4–8.4)	BMM	2.6
OAK-02–172	9.43×10^{-1} (±1%)	2.12×10^{-2} (±1%)	0.02 (±31%)	1.63 (±3%)	7.8 (7.2–8.4)	6.1 (5.2–7.0)	2.06 (1.94–2.20)	3.2 (3.1–3.3)	0.20	21.2	11.3	n/a	20.4 (20.0–21.4)	PFM	<0.1
OAK-03–15	8.27×10^{-1} (±1%)	1.91×10^{-2} (±1%)	2.38 (±0.1%)	3.01 (±3%)	5.8 (5.2–6.4)	9.4 (8.5–10.4)	4.71 (4.40–5.05)	426.2 (361.9–448.0)	0.15	4.4	2.1	0.76 (0.75–0.83)	1.9 (0.5–4.9)	BMM	5.5
OAK-04–59	8.50×10^{-1} (±1%)	1.96×10^{-2} (±1%)	0.40 (±1.3%)	0.33 (±3%)	5.9 (5.4–6.4)	8.2 (7.3–9.1)	0.50 (0.47–0.53)	67.4 (64.0–70.5)	0.15	22.8	9.8	0.13 (0.11–0.13)	12.4 (9.1–13.5)	BMM	<0.1
OAK-04–89	9.93×10^{-1} (±1%)	1.99×10^{-2} (±1%)	0.03 (±22.7%)	0.99 (±3%)	7.2 (6.6–7.8)	8.7 (7.7–9.7)	1.38 (1.29–1.47)	5.0 (4.7–5.3)	0.12	22.5	18.7	n/a	24.9 (24.0–25.4)	PFM	2.3
ASH-01–50	8.57×10^{-1} (±1%)	2.08×10^{-2} (±1%)	4.54 (±0.1%)	3.42 (±3%)	4.4 (3.8–4.9)	4.3 (3.5–5.1)	5.07 (4.74–5.40)	630.4 (601.4–660.0)	0.20	36.1	11.7	n/a	6.9 (5.5–8.4)	PFM	4.6
ASH-02–59	7.07×10^{-1} (±1%)	1.87×10^{-2} (±1%)	2.86 (±1.5%)	2.13 (±3%)	0.5 (0.1–1.0)	5.2 (4.5–6.0)	4.41 (4.06–4.75)	430.0 (409.3–446.7)	0.20	54.1	2.7	0.78 (0.75–0.82)	6.4 (1.9–7.4)	BMM	4.9
ASH-03–108	7.10×10^{-1} (±1%)	1.80×10^{-2} (±1%)	0.25 (±3.2%)	0.72 (±3%)	1.9 (1.4–2.4)	8.2 (7.4–9.0)	1.48 (1.38–1.61)	43.1 (41.5–45.4)	0.20	51.3	0.8	n/a	24 (23.4–25.0)	PFM	0.1
ASH-05–15	8.35×10^{-1} (±1%)	1.57×10^{-2} (±1%)	0.30 (±2.1%)	2.26 (±3%)	1.5 (1.0–2.0)	14.3 (13.3–15.2)	5.89 (5.36–6.48)	69.6 (66.2–72.9)	0.20	12.1	1.8	n/a	3.4 (0.4–5.5)	PFM	5.1
ASH-06–59	6.29×10^{-1} (±1%)	1.61×10^{-2} (±1%)	20.48 (±0.2%)	1.01 (±3%)	1.2 (0.8–1.6)	12.2 (11.4–13.1)	2.56 (2.38–2.78)	4378.9 (4172.2–4555.5)	0.20	13.2	1.2	n/a	18 (16.9–19.1)	PFM	16.6
FIR-04–40	7.14×10^{-1} (±1%)	1.71×10^{-2} (±1%)	2.57 (±0.5%)	2.16 (±3%)	3.6 (3.2–4.1)	12.1 (11.2–13.0)	4.31 (4.02–4.60)	529.7 (510.1–559.1)	0.10	5.9	3.6	0.96 (0.93–1.0)	9.4 (7.6–11.4)	BMM/PFM	3.6
FIR-06–40	5.81×10^{-1} (±1%)	1.52×10^{-2} (±1%)	2.38 (±0.7%)	2.39 (±3%)	0.5 (0.2–0.8)	13.9 (13.1–14.8)	7.07 (6.54–7.63)	558.2 (530.4–577.2)	0.10	2.5	1.0	n/a	∼0	PFM	5.7
FIR-07–35	6.45×10^{-1} (±1%)	1.68×10^{-2} (±1%)	2.55 (±0.9%)	2.22 (±3%)	0.7 (0.3–1.1)	9.6 (8.8–10.4)	5.39 (4.98–5.86)	481.6 (461.2–502.9)	0.10	47.3	1.0	0.89 (0.85–0.92)	2.4 (1.4–5.1)	BMM	6.6
FIR-07–63	7.49×10^{-1} (±1%)	1.81×10^{-2} (±1%)	1.97 (±1.2%)	0.90 (±3%)	3.6 (3.1–4.1)	9.5 (8.6–10.4)	1.66 (1.55–1.79)	363.8 (343.6–378.2)	0.20	47.3	10.3	0.76 (0.66–0.77)	19.9 (17.4–23.5)	BMM/PFM	8.0
FIR-08–86	7.12×10^{-1} (±1%)	1.74×10^{-2} (±1%)	0.94 (±1.8%)	0.66 (±3%)	3.1 (2.4–3.6)	10.8 (9.9–11.7)	1.32 (1.24–1.43)	185.4 (175.2–192.6)	0.20	59.2	2.5	0.34 (0.32–0.35)	12.4 (9.9–14.0)	BMM	7.3

[a]Sample ID codes (e.g., OAK-02–34) reflect study area name, well location, and unique field identifier number. BMM = binary mixing model; PFM = piston flow model.

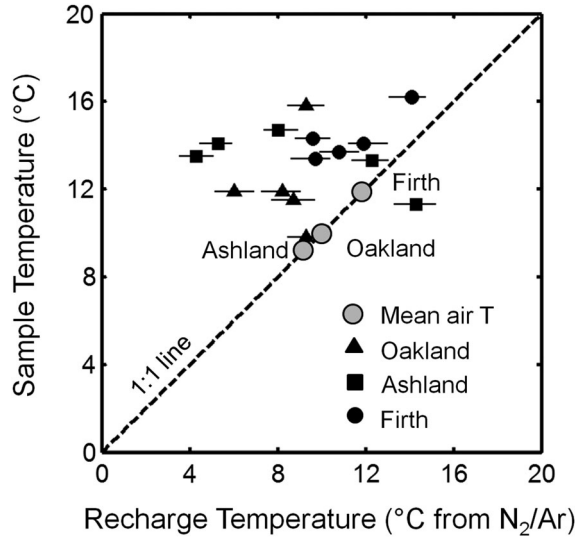

Figure 7. Scatterplot of sample temperatures (measured at the wellhead at the time of sample collection) and recharge temperatures from N_2 and Ar (corrected for excess air and assuming recharge elevation equal to sample elevation). Mean annual air temperatures also shown.

topography and layered soils are scarce. Also, the extent to which focused versus diffuse recharge mechanisms in the study area would affect unsaturated-zone lag times for CFCs and SF_6 is unclear. While the regional median unsaturated-zone thickness is ~26 m, the majority of well sites in this study have local water tables <10 m below surface. Therefore, the recharge calculations in this study assume that CFC-12 and SF_6 tracer ages reflect residence times in the saturated zone. Samples shown in Figure 8 within the 2–6 year binary mixing model space are not highly sensitive to unsaturated zone time lags because of their short residence times. Three samples with higher apparent ages (FIR-07–63, FIR-04–40, and OAK-04–59) had water tables <10 m below land surface. FIR-08–86 has the highest likelihood of significant age

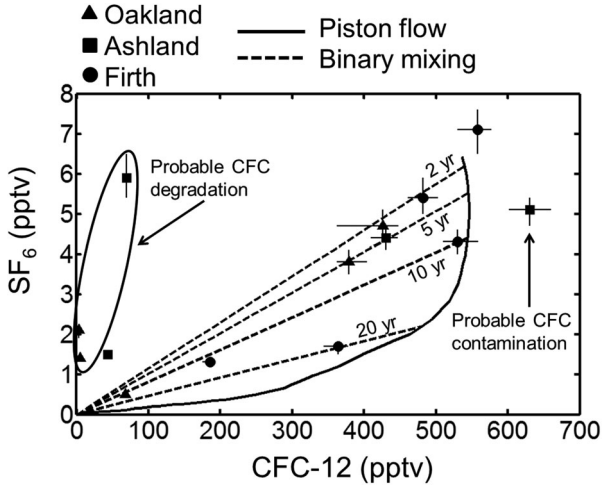

Figure 8. Tracer plot for CFC-12 and SF_6. Model curves shown for piston flow and binary mixing with young water fraction ages between 2 and 20 years. ASH-06–59 not shown (out of range on the CFC-12 axis; see Table 3).

bias because of the water-table depth of 22 m and relatively high residence time, which would manifest in overestimation of residence time and underestimation of recharge rate.

[32] Groundwater tracer-based recharge rates were calculated from mixing model solutions and estimates of porosity and saturated thickness developed from local well logs (Table 5). Recharge estimates range from 6 mm yr^{-1} (ASH-03–108; 1σ range 6–7 mm yr^{-1}) to 409 mm yr^{-1} (ASH-01–50; 1σ range 276–516 mm yr^{-1}) (Table 5). The 409 mm yr^{-1} value for ASH-01–50 is an outlier equal to more than twice the next largest rate that is likely affected by stream seepage given its proximity to the active Platte River channel. When this sample is excluded, the median recharge rate from environmental tracers is 58 mm yr^{-1}. Error ranges tended to be lowest for samples with low recharge rates, but exceeded 100% of the rate estimate in several samples with relatively high recharge rates (Table 5). The subset of recharge rates estimated from samples without CFC-12 degradation or contamination are considered to be the most reliable given that mixing model fits could be assessed from two tracers. The median recharge rate from this subset was 56 mm yr^{-1}, in good agreement with the central tendency of the overall data set when ASH-01–50 is excluded.

4.3. Regional-Scale Recharge

[33] The spatially weighted mean recharge rate for the glaciated study region (Figure 1) was extracted from the statewide data set presented by *Szilagyi and Jozsa* [2012] for 2000–2009. A value of 56 mm yr^{-1} was obtained for this period (1σ range 14–91 mm yr^{-1}). This rate is within ~4% of the groundwater tracer-based estimate of 58 mm yr^{-1} when the high-recharge outlier ASH-01–50 is excluded. This value also compares favorably with recharge estimates from the same area by *Nolan et al*. [2007], who report 27 groundwater (saturated zone) chloride-based recharge rates with a median of 53 mm yr^{-1}.

4.4. Comparison Across Nested Spatial Scales

4.4.1. Consistency With Lithological Controls on Recharge Through Incised Glacial Till

[34] Profile-scale recharge estimates were developed for one site where glacial till was absent (OAK-03-UZ) and two sites where glacial till was present (ASH-02-UZ and FIR-04-UZ); contrasting results across these sites illustrates the lithologic influence on recharge processes (Table 5). The ASH-02-UZ unsaturated zone profile time series provides an illustration of the role of low permeability till in limiting upland recharge. Essentially all soil-water dynamics were limited to the top 4 m of the profile above a low-conductivity till layer. The low matric potentials and low recharge estimate for ASH-02-UZ below the till layer suggests that negligible recharge took place through the till at this location. At the second till-present site (FIR-04-UZ), wetting fronts below the root zone occur intermittently, but this drainage contributes to a local perched aquifer, rather than to regional groundwater. Only the monitoring results for the till-absent site (OAK-03-UZ) show wetting fronts reaching the regional water table. Comparisons of recharge rates between OAK-03-UZ (to the regional water table) and FIR-04-UZ (to the local perched aquifer) are equivocal because of the substantial difference in FIR-04-UZ

Table 4. Redox Indicator Data for Groundwater Samples[a]

Sample	O_2	NO_3–N	Fe^{2+}	Mn^{2+}	SO_4^{2-}	CH_4
ASH-02-59	n/a	n/a	n/a	n/a	n/a	n/a[c]
FIR-07-35	6.6[b]	<0.2	0.16	0.01	11	<0.005[c]
OAK-02-34	6.8	16.5	0.02	<0.01	30	<0.005[c]
OAK-03-15	2.8	7.6	0.02	<0.01	14	<0.005[c]
ASH-01-50	<0.1	<0.2	0.02	1.32	71	0.003[c]
ASH-06-59	6.3	17	0.02	<0.01	28	<0.005[c]
ASH-03-108	4.9	7.2	0.01	<0.01	54	<0.005[c]
ASH-05-15	<0.1	0.9	0.04	0.16	108	0.011[c]
OAK-02-172	0.2	0.2	0.03	0.22	157	<0.005[c]
OAK-04-89	1.7	<0.2	1.18	2.01	34	0.029[c]
FIR-08-86	8.2	8.9	0.02	<0.01	14	<0.005[c]
OAK-04-59	0.6	<0.2	1.98	1.83	13	0.110[c]
FIR-04-40	5.5	101	0.02	0.52	46	<0.005[c]
FIR-07-63	8.4	3.7	0.02	<0.01	24	0.041[c]
FIR-06-40	9.9[b]	23.4	<0.01	<0.01	73	<0.005[c]

[a]All concentrations are expressed as mg/L. Data are from closest available measurement period to the collection date of age-dating samples during May-June 2009. Data are from Febuary 2009 unless otherwise noted.
[b]Denotes sample collected September-November 2008.
[c]Denotes sample collected May-June 2009.

recharge estimates ranges across methodologies. Discrepancies in Cl^- (2–8 mm yr^{-1}) and ^3H (25–43 mm yr^{-1}) tracer mass balance estimates at FIR-04-UZ may be associated with larger than anticipated uncertainties in deposition rates, or may reflect the positive bias in ^3H-based recharge estimates that has been observed in some unsaturated zones with low drainage rates [*Cook et al*., 1994]. FIR-04-UZ recharge estimates from matric potentials and Cl^- mass balance are in better agreement, and would suggest that recharge rates to the perched water table at this site are lower than recharge rates to the regional water table OAK-03-UZ. Also, when comparing FIR-04-UZ and OAK-03-UZ, it should be noted that the recharge rate at OAK-03-UZ may have been lower than the regional average partly because of the relatively shallow water table. During the study monitoring period, the water table depth at OAK-03-UZ was ~3 m below surface, which is within a range that may experience significant groundwater evapotranspiration. For example, net groundwater recharge rates in the Platte River valley (which overlaps with this study area) were found to transition between negative and positive values at a water table depth of 2 ± 1 m [*Szilagyi et al*., 2012]. Water potential gradient reversals during the monitoring period suggest that transient discharge occurs at this location.

[35] Because detailed till lithology is only available for smaller subareas within the study region, unsaturated zone thickness is used as a proxy indicator of regional till cover in order to assess lithological controls on recharge on the regional scales. The assumption should be reasonable given that percent till abundance has been shown to generally increase with increasing unsaturated zone thickness [*Divine and Korus*, 2012]. Figure 9 shows the relationship between unsaturated zone thickness and recharge estimates from groundwater ages. Although uncertainty ranges are large and overlapping for several samples, particularly for relatively shallow samples with recharge estimates >50 mm/yr, 13 of the 14 samples that yielded recharge estimates are generally consistent with a trend of declining recharge rate with increasing unsaturated zone thickness. Even when the ASH-01–50 outlier is removed, the central tendency points toward a predominantly negative relationship between topographic position and recharge rate (two-tail Kendall tau value is -0.42 with $p = 0.06$). The outlier in Figure 9 (OAK-02–172) with apparently high recharge (148 mm yr^{-1}) is one in which CFC-12 degradation prevented mixing model interpretation of tracer ages, and therefore, recharge was estimated with SF_6 and the piston flow model based on the criteria described in section 3.3.3. However, this sample also had one of only two ^3H nondetects, which is not consistent with the SF_6-estimated mean residence time of 20 years, suggesting that the piston flow model may have resulted in positive recharge bias in this case.

[36] To evaluate relationships between recharge and unsaturated zone thickness on the regional scale, water-balance model estimates [*Szilagyi and Jozsa*, 2012] were aggregated into mean recharge rates for unsaturated-zone

Table 5. Recharge Rate Estimates (All Sites and Methods)

Site	q (mm yr^{-1})	Method
Profile Scale		
OAK-03-UZ	21 (10–36)	Buckingham-Darcy
ASH-02-UZ	0.0001	Buckingham-Darcy
FIR-04-UZ	9 (4–12)	Buckingham-Darcy
FIR-04-UZ	5 (2–8)	Chloride mass balance
FIR-04-UZ	34 (25–43)	Tritium mass balance
Aquifer Scale		
OAK-02-34	58 (30–161)	CFC-12/SF_6
OAK-02-172	158 (106–161)	SF_6
OAK-03-15	127 (52–659)	CFC-12/SF_6
OAK-04-59	20 (14–23)	CFC-12/SF_6
OAK-04-89	193 (88–200)	SF_6
ASH-01-50	409 (276–516)	SF_6
ASH-02-59	73 (61–224)	CFC-12/SF_6
ASH-03-108	7 (6–7)	SF_6
ASH-05-15	104 (65–960)	SF_6
ASH-06-59	13 (12–15)	SF_6
FIR-04-40	57 (31–67)	CFC-12/SF_6
FIR-07-35	37 (18–66)	CFC-12/SF_6
FIR-07-63	89 (73–99)	CFC-12/SF_6
FIR-08-86	14 (13–17)	CFC-12/SF_6
Regional Scale		
n/a	56 (14–91)	Water Balance Model

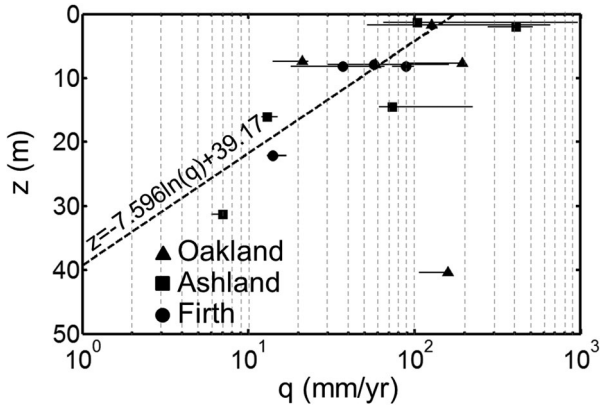

Figure 9. Scatter plot of unsaturated zone thicknesses and apparent recharge rates from mean groundwater-tracer ages.

thickness bins with 10 m increments. Grid cells showing net negative recharge are omitted from the reported recharge statistics because they represent discharge zones. Results show a regional trend of declining recharge rates with increasing unsaturated zone thickness that is qualitatively similar to the field results (Figure 10). Data points on Figure 10 represent spatial averages of areas ranging from 192 to 9480 km^2.

4.4.2. Diffuse Versus Nondiffuse Recharge Mechanisms Through Incised Glacial Till

[37] Recharge estimates based on unsaturated zone measurements (five separate estimates from three sites using three methods) were all lower than the regional and aquifer scale recharge estimates (water balance model median recharge rate from groundwater tracers; Figure 11 and Table 5). One possible explanation for this difference

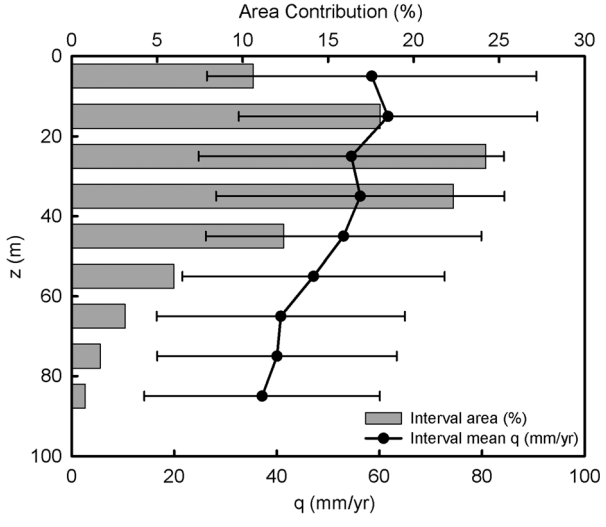

Figure 10. Recharge results of water-balance modeling for eastern Nebraska glaciated region (the region denoted in grey in the top-left index map within Figure 1) as a function of unsaturated zone thickness. Gray bars show percent area of the region with corresponding unsaturated zone thicknesses.

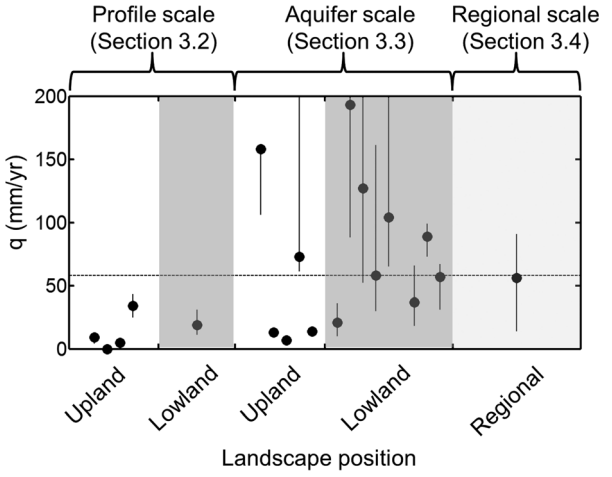

Figure 11. Recharge estimate comparison by method and setting. Horizontal broken line shows median value of groundwater ages from CFC-12 and SF_6.

is that nondiffuse recharge processes that do not significantly affect drainage rates at the three profile monitoring sites contribute to recharge at other locations, for example through fracture flow or ponding, thereby affecting aquifer-scale and regional recharge estimates. Several previous studies have found that overland flow can significantly enhance recharge rates in topographic lows [*Derby and Knighton*, 2001; *Scanlon and Goldsmith*, 1997], and preferential flow has been shown to significantly affect recharge rates through till in some settings [*Jørgensen et al*., 2002; *Nilsson et al*., 2001].

[38] While no direct field evidence of nondiffuse recharge mechanisms is available in the current study, a comparison of unsaturated zone and groundwater-based recharge estimates may provide preliminary constraints on the importance of diffuse versus nondiffuse recharge mechanisms. For example, if total recharge (diffuse plus nondiffuse) is within the range of 56–58 mm yr^{-1} (as estimated by the regional water balance model and the median estimate from groundwater tracers), and diffuse recharge is within the range of recharge rates obtained from the five unsaturated zone methods (0–43 mm yr^{-1} including uncertainty bounds), estimates of diffuse recharge as a percentage of total recharge would range from 0% to a maximum 61%. However, zero regional diffuse recharge does not provide a satisfactory lower bound because glacial till is absent from ~35% of the study region. To provide a more reasonable lower bound, assume that the Cl^- mass balance estimate of 5 mm yr^{-1} (FIR-04-UZ) is applied to the till-covered percentage of the region (65%), and the lowland Buckingham-Darcy estimate of 21 mm yr^{-1} (OAK-03-UZ) is applied to the till-absent percentage of the region (35%). Under this assumption, the minimum estimate of diffuse recharge as a percentage of total recharge would be 18%. In all cases, estimates of diffuse recharge do not exceed about 60% for any combination of recharge estimates developed in this study, underscoring the likely importance of nondiffuse recharge in this landscape. However, it is emphasized that these estimates are subject to high uncertainty stemming from the limited number of measurements, incongruities in both spatial and temporal time scales

between groundwater and unsaturated zone-based estimates, lack of unsaturated zone monitoring sites in locations receiving overland flow or ponding, and potential for unknown biases not taken into account in tracer interpretations. Further investigations are necessary to elucidate the processes leading to nondiffuse recharge in this region.

5. Summary and Conclusions

[39] This study provides groundwater recharge estimates for an incised glacial landscape on nested plot, aquifer, and regional scales using a combination of chemical and physical methods. The primary goal was to evaluate the extent to which recharge rates reflect lithologic influences. Despite substantial uncertainties associated with each recharge estimate method, lithologic influences on recharge rates were indicated on all scales. Key results are as follows.

[40] Diffuse recharge to paleovalley aquifers was prevented by perching above glacial till at both upland unsaturated zone monitoring sites. At one upland site, recharge estimates to the local perched aquifer developed from matric potentials, pore water Cl^-, and ^3H were 9, 5, and 34 mm yr^{-1}, respectively. Diffuse recharge at a lowland site with till absent due to river incision averaged 21 mm yr^{-1} to a regional water table ~3 m below surface for 2008–2012 based on matric potentials. Total recharge (diffuse plus nondiffuse) for the three study sites was estimated to be 58 mm yr^{-1} based on the median value of 14 estimates developed from CFC-12 and SF_6 in groundwater. Total recharge for the eastern Nebraska glaciated region averaged 56 mm yr^{-1} based on a remote sensing-assisted water-balance model. The good correspondence between the two estimates adds confidence that recharge conditions within the selected field study areas were broadly representative of the region.

[41] A negative relationship between recharge rate and unsaturated zone thickness is evident on the profile scale (matric potential monitoring and unsaturated chemical zone tracers), aquifer scale (groundwater dating), and regional scale (remote sensing-assisted water balance model). The negative relationship is interpreted to reflect the fact that higher recharge rates are associated with areas where fine-grained glacial till is absent, given that these areas primarily coincide with lowlands where river incision has removed till deposits. Area-weighted averaging of recharge rates through upland and lowland areas suggests that a maximum of ~60% of total recharge is from diffuse sources, implying that indirect recharge processes through preferential flow conduits or focused recharge in topographic lows receiving overland flow, which were not measured in this study, may represent an important component of the regional groundwater budget.

[42] The results of this study also help to constrain recharge rates to glacial aquifers in the eastern Great Plains region for groundwater management purposes. From a water resources management perspective, a distinction should be made between recharge to local upland perched aquifers and underlying alluvial or paleovalley aquifers. While perching above till layers may largely prevent diffuse recharge to underlying units, the overlying perched aquifer systems may be sustainable as locally valuable irrigation or drinking-water supplies in some cases.

[43] **Acknowledgments.** We acknowledge the financial support of the Eastern Nebraska Water Resources Assessment project and its sponsoring organizations and cooperative agencies (Lewis and Clark NRD, Lower Elkhorn NRD, Papio-Missouri River NRD, Lower Platte North NRD, Lower Platte South NRD, Nemaha NRD, Nebraska Department of Natural Resources, University of Nebraska Conservation and Survey Division, and U.S. Geological Survey). Valuable suggestions and field contributions were provided by Dana Divine and Karen Griffin. Any use of trade, firm, or product names is for descriptive purposes only and does not imply endorsement by the U.S. Government.

References

Abraham, J. D., P. A. Bedrosian, T. H. Asch, L. B. Ball, J. C. Cannia, J. D. Phillips, and S. Lackey (2012), Evaluation of geophysical techniques for the detection of paleochannels in the Oakland area of eastern Nebraska as part of the Eastern Nebraska Water Resource Assessment, *U.S. Geol. Surv. Sci. Invest. Rep. 2011–5228*, 40 pp.

Aeschbach-Hertig, W., F. Peeters, U. Beyerle, and R. Kipfer (2000), Paleotemperature reconstruction from noble gases in ground water taking into account equilibrium with entrapped air, *Nature*, *405*, 1040–1044.

Alcamo, J., P. Döll, T. Henrichs, F. Kaspar, B. Lehner, T. Rosch, and S. Siebert (2003), Development and testing of the WaterGAP 2 global model of water use and availability, *Hydrol. Sci. J.*, *48*(3), 317–337.

Aller, L., T. Bennett, J. H. Lehr, and R. J. Petty (1987), DRASTIC: A standardized system for evaluating groundwater pollution potential using hydrogeologic settings, *U. S. Environ. Protect. Agency Rep., EPA/600/2–85-018*, Natl. Water Well Assoc., Dublin, Ohio.

Allison, G. B., and M. W. Hughes (1978), The use of environmental tritium and chloride to estimate total recharge to an unconfined aquifer, *Aust. J. Soil Sci.*, *16*, 181–195.

Böhlke, J. K. (2002), Groundwater recharge and agricultural contamination, *Hydrgeol. J.*, *10*, 153–179.

Brock, F. V., K. C. Crawford, R. L. Elliott, G. W. Cuperus, S. J. Stadler, H. L. Johnson, and M. D. Eilts (1995), The Oklahoma Mesonet: A technical overview, *J. Atmos. Oceanic Technol.*, *12*(1), 5–19.

Busenberg, E., L. N. Plummer, and R. C. Bartholomay (2001), Estimated age and source of the young fraction of ground water at the Idaho National Engineering and Environmental Laboratory, *U.S. Geol. Surv. Water-Resour. Invest. Rep. 01-4265*, 144 pp.

Busenberg, E., L. N. Plummer, P. G. Cook, D. K. Solomon, L. F. Han, M. Groning, and H. Oster (2006), *Use of Chlorofluorocarbons in Hydrology: A Guidebook, STI/PUB/1238*, 277 pp., Int. At. Energy Agency.

Cook, P., and J. K. Böhlke (2000), Determining timescales for groundwater flow and solute transport, in *Environmental Tracers in Subsurface Hydrology*, edited by P. Cook and A. Herczeg, pp. 1–30, Kluwer, Boston.

Cook, P. G., and D. K. Solomon (1995), Transport of atmospheric trace gases to the water table: Implications for groundwater dating with chlorofluorocarbons and krypton 85, *Water Resour. Res.*, *31*(2), 263–270.

Cook, P. G., G. R. Walker, G. Buselli, I. Potts, and A. R. Dodds (1992), The application of electromagnetic techniques to groundwater recharge investigations, *J. Hydrol.*, *130*(1–4), 201–229.

Cook, P. G., I. D. Jolly, F. W. Leaney, G. R. Walker, G. L. Allan, L. K. Fifield, and G. B. Allison (1994), Unsaturated zone tritium and chlorine 36 profiles from southern Australia: Their use as tracers of soil water movement, *Water Resour. Res.*, *30*(6), 1709–1719.

Cook, P. G., F. W. Leaney, and I. D. Jolly (2001), Groundwater recharge in the Mallee region, and salinity implications for the Murray River: A Review, *Tech. Rep. 45/01*, CSIRO Land and Water, Glen Osmond, Australia.

Cuthbert, M. O., R. Mackay, J. H. Tellam, and K. E. Thatcher (2010), Combining unsaturated and saturated hydraulic observations to understand and estimate groundwater recharge through glacial till, *J. Hydrol.*, *391*(3–4), 263–276.

Daniels, D. P., S. J. Fritz, and D. I. Leap (1991), Estimating recharge rates through unsaturated glacial till by tritium tracing, *Ground Water*, *29*(1), 26–34.

Darling, W. G., D. C. Gooddy, A. M. MacDonald, and B. L. Morris (2012), The practicalities of using CFCs and SF6 for groundwater dating and tracing, *Appl. Geochem.*, *27*(9), 1688–1697.

Delin, G. N., R. W. Healy, D. L. Lorenz, and J. R. Nimmo (2007), Comparison of local- to regional-scale estimates of ground-water recharge in Minnesota, USA, *J. Hydrol.*, *334*(1–2), 231–249.

Derby, N. E., and R. E. Knighton (2001), Field-scale preferential transport of water and chloride tracer by depression-focused recharge, *J. Environ. Qual.*, *30*(1), 194–199.

de Vries, J., and I. Simmers (2002), Groundwater recharge: An overview of processes and challenges, *Hydrogeol. J.*, *10*(1), 5–17.

Divine, D. P., and J. T. Korus (2012), *Three-Dimensional Hydrostratigraphy of the Sprague, Nebraska Area: Results From Helicopter Electromagnetic (HEM) Mapping for the Eastern Nebraska Water Resources Assessment (ENWRA), Conserv. Bull. 4 (New Ser.)*, Conserv. and Surv. Div., Sch. of Nat. Resour., Univ. of Nebraska-Lincoln, Lincoln, Neb.

Divine, D. P., R. M. Joeckel, J. T. Korus, P. R. Hanson, and S. O. Lackey (2009), *Eastern Nebraska Water Resources Assessment (ENWRA), Introduction to a Hydrogeological Study, Conserv. Bull. 1 (New Ser.)*, Conserv. and Sur. Div., Sch. of Nat. Resour., Univ. of Nebraska-Lincoln, Lincoln, Neb.

Döll, P., and K. Fiedler (2007), Global-scale modeling of groundwater recharge, *Hydrol. Earth Syst. Sci.*, *4*, 4069–4124.

Dripps, W., and K. Bradbury (2007), A simple daily soil–water balance model for estimating the spatial and temporal distribution of groundwater recharge in temperate humid areas, *Hydrogeol. J.*, *15*(3), 433–444.

Eberts, S. M., J. K. Böhlke, L. J. Kauffman, and B. C. Jurgens (2012), Comparison of particle-tracking and lumped-parameter age-distribution models for evaluating vulnerability of production wells to contamination, *Hydrogeol. J.*, *20*(2), 263–282.

Edmunds, W. M. (2010), Conceptual models for recharge sequences in arid and semi-arid regions using isotopic and geochemical methods, in *Groundwater Modeling in Arid and Semi-Arid Areas*, edited by H. S. Wheater, S. A. Mathias, and X. Li, pp. 21–38, Cambridge Univ, Press, Cambridge, U. K.

Engesgaard, P., A. L. Højberg, K. Hinsby, K. H. Jensen, T. Laier, F. Larsen, E. Busenberg, and L. N. Plummer (2004), Transport and time lag of chlorofluorocarbon gases in the unsaturated zone, Rabis Creek, Denmark, *Vadose Zone J.*, *3*(4), 1249–1261.

Entekhabi, D., and M. Moghaddam (2007), Mapping recharge from space: Roadmap to meeting the grand challenge, *Hydrogeol. J.*, *15*(1), 105–116.

Espeby, B. (1992), Coupled simulations of water flow from a field-investigated glacial till slope using a quasi-two-dimensional water and heat model with bypass flow, *J. Hydrol.*, *131*(1–4), 105–132.

Feddes, R. A., P. Kabat, P. J. T. Van Bakel, J. J. B. Bronswijk, and J. Halbertsma (1988), Modelling soil water dynamics in the unsaturated zone: State of the art, *J. Hydrol.*, *100*(1–3), 69–111.

Flint, A. L., G. S. Campbell, K. M. Ellett, and C. Calissendorff (2002), Calibration and temperature correction of heat dissipation matric potential sensors, *Soil Sci. Soc. Am. J.*, *66*(5), 1439–1445.

Gates, J. B., W. M. Edmunds, W. G. Darling, J. Ma, Z. Pang, and A. A. Young (2008), Conceptual model of recharge to southeastern Badain Jaran Desert groundwater and lakes from environmental tracers, *Appl. Geochem.*, *23*(12), 3519–3534.

Gates, J. B., B. Scanlon, X. Mu, and L. Zhang (2011), Impacts of soil conservation on groundwater recharge in the semi-arid Loess Plateau, China, *Hydrogeol. J.*, *19*(4), 865–875.

Gerber, R. E., and K. W. F. Howard (1996), Evidence for recent groundwater flow through Late Wisconsinan till near Toronto, Ontario, *Can. Geotech. J.*, *33*(4), 538–555.

Gerber, R. E., and K. Howard (2000), Recharge through a regional till aquitard: Three-dimensional flow model water balance approach, *Ground Water*, *38*(3), 410–422.

Gosselin, D. C., J. Headrick, X. H. Chen, S. E. Summerside, R. Tremblay, and K. Bottger (1996), Domestic well-water quality in rural Nebraska, *Data Anal. Rep*., Conserv. and Surv. Div., Univ. of Nebraska-Lincoln, Lincoln, Neb.

Gosselin, D. C., F. E. Harvey, and C. A. Flowerday (2003), The complex Dakota aquifer: Managing groundwater in Nebraska, *Geotimes*. [Available at http://www.geotimes.org/apr03/feature_nebraska.html.]

Gurdak, J. J., R. T. Hanson, P. B. McMahon, B. W. Bruce, J. E. McCray, G. D. Thyne, and R. C. Reedy (2007), Climate variability controls on unsaturated water and chemical movement, High Plains Aquifer, USA, *Vadose Zone J.*, *6*, 533–547.

Harvey, F. E., J. F. Ayers, and D. C. Gosselin (2007), Ground water dependence of endangered ecosystems: Nebraska's eastern saline wetlands, *Ground Water*, *45*(6), 736–752.

Healy, R. W. (2010), *Estimating Groundwater Recharge*, Cambridge Univ. Press, Cambridge, U. K.

Heilweil, V., and K. Solomon (2004), Millimeter- to kilometer-scale variations in vadose-zone bedrock solutes: Implications for estimating recharge in arid settings, in *Groundwater Recharge in a Desert Environment: The Southwestern United States*, edited by J. F. Hogan, F. Phillips, and B. R. Scanlon, pp. 235–254, AGU, Washington, D. C.

Hendry, M. J. (1983), Groundwater recharge through a heavy-textured soil, *J. Hydrol.*, *63*(3–4), 201–209.

Hendry, M. J. (1988), Hydrogeology of clay till in a Prairie region of Canada, *Ground Water*, *26*(5), 607–614.

Hendry, M. J., C. J. Kelln, L. I. Wassenaar, and J. Shaw (2004), Characterizing the hydrogeology of a complex clay-rich aquitard system using detailed vertical profiles of the stable isotopes of water, *J. Hydrol.*, *293*(1–4), 47–56.

Hinsby, K., A. L. Højberg, P. Engesgaard, K. H. Jensen, F. Larsen, L. N. Plummer, and E. Busenberg (2007), Transport and degradation of chlorofluorocarbons (CFCs) in the pyritic Rabis Creek aquifer, Denmark, *Water Resour. Res.*, *43*, W10423, doi:10.1029/2006WR005854.

Jørgensen, F., and P. B. E. Sandersen (2006), Buried and open tunnel valleys in Denmark: Erosion beneath multiple ice sheets, *Quat. Sci. Rev.*, *25*(11–12), 1339–1363.

Jørgensen, P. R., M. Hoffmann, J. P. Kistrup, C. Bryde, R. Bossi, and K. G. Villholth (2002), Preferential flow and pesticide transport in a clay-rich till: Field, laboratory, and modeling analysis, *Water Resour. Res.*, *38*(11), 1246, doi:10.1029/2001WR000494.

Jurgens, B. C., J. K. Böhlke, and S. M. Eberts (2012), TracerLPM (Version 1): An Excel® workbook for interpreting groundwater age distributions from environmental tracer data, *U.S. Geol. Surv. Tech. Methods Rep., 4-F3*, 60 p.

Jyrkama, M. I., and J. F. Sykes (2007), The impact of climate change on spatially varying groundwater recharge in the grand river watershed (Ontario), *J. Hydrol.*, *338*(3–4), 237–250.

Keese, K. E., B. R. Scanlon, and R. C. Reedy (2005), Assessing controls on diffuse groundwater recharge using unsaturated flow modeling, *Water Resour. Res.*, *41*, W06010, doi:10.1029/2004WR003841.

Kehew, A. E., and W. M. Boettger (1986), Depositional environments of buried-valley aquifers in North Dakota, *Ground Water*, *24*(6), 728–734.

Kehew, A. E., J. A. Piotrowski, and F. Jørgensen (2012), Tunnel valleys: Concepts and controversies: A review, *Earth Sci. Rev.*, *113*(1–2), 33–58.

Kehew, A. E., S. K. Ewald, J. M. Esch, and A. L. Kozlowski (2013), On the origin of tunnel valleys of the Saginaw Lobe of the Laurentide Ice Sheet; Michigan, USA, *Boreas*, *42*(2), 442–462.

Kim, J. H., and R. B. Jackson (2012), A global analysis of groundwater recharge for vegetation, climate, and soils, *Vadose Zone J.*, *11*(1), doi: 10.2136/vsj2011.0021RA.

Klute, A. (1986), Water retention: Laboratory methods, in *Methods of Soil Analysis: Part 1: Physical and Mineralogical Methods*, edited by A. Klute, pp. 635–662, Am. Soc. of Agron., Soil Sci. Soc. of Am., Madison.

Korus, J. T., R. M. Joekel, and D. P. Divine (2013), *Three-Dimensional Hydrostratigraphy of the Firth, Nebraska Area: Results From Helicopter Electromagnetic (HEM) Mapping in the Eastern Nebraska Water Resources Assessment (ENWRA), Conserv. Bull. 3 (New Ser.)*, 100 p., Conserv. and Surv. Div., Sch. of Nat. Resour., Inst. of Agric. and Nat. Resour., Univ. of Nebraska-Lincoln, Lincoln, Neb.

Lerner, D. N., A. S. Isaar, and I. Simmers (Eds.) (1990), Groundwater recharge: A guide to understanding and estimating natural recharge, in *International Contributions to Hydrogeology*, vol. 8, Verlag Heinz Heise, Hanover, Germany.

Maloszewski, P., and A. Zuber (1996), Lumped parameter models for the interpretation of environmental tracer data, in *Manual on Mathematical Models in Isotope Hydrogeology, TECDOC-910*, pp. 9–58, Int. At. Energy Agency, Vienna.

Manning, A. H., and J. S. Caine (2007), Groundwater noble gas, age, and temperature signatures in an Alpine watershed: Valuable tools in conceptual model development, *Water Resour. Res.*, *43*, W04404, doi: 10.1029/2006WR005349.

Massoudieh, A., S. Sharifi, and D. K. Solomon (2012), Bayesian evaluation of groundwater age distribution using radioactive tracers and anthropogenic chemicals, *Water Resour. Res.*, *48*, W09529, doi:10.1029/2012 WR011815.

McMahon, P. B., L. N. Plummer, J. K. Böhlke, S. D. Shapiro, and S. R. Hinkle (2011), A comparison of recharge rates in aquifers of the United States based on groundwater-age data, *Hydrogeol. J.*, *19*(4), 779–800.

Michel, R. L. (2005), Tritium in the hydrologic cycle, in *Isotopes in the Water Cycle: Past, Present and Future of a Developing Sciences*, edited by P. K. Aggarwal, J. R. Gat, and K. F. O. Froehlich, pp. 53–66, Int. At. Energy Agency, Vienna.

Nasta, P., and J. B. Gates (2013), Plot-scale modeling of soil water dynamics and impacts of drought conditions beneath rainfed maize in Eastern Nebraska, *Agric. Water Manage.*, *128*, 120–130.

Ng, G.-H. C., D. McLaughlin, D. Entekhabi, and B. Scanlon (2009), Using data assimilation to identify diffuse recharge mechanisms from chemical and physical data in the unsaturated zone, *Water Resour. Res.*, *45*, W09409, doi:10.1029/2009WR007831.

Nielsen, D. R., M. T. van Genuchten, and J. W. Biggar (1986), Water flow and solute transport processes in the unsaturated zone, *Water Resour. Res.*, *22*(9), 89S–108S.

Nilsson, B., R. C. Sidle, K. E. Klint, C. E. Bøggild, and K. Broholm (2001), Mass transport and scale-dependent hydraulic tests in a heterogeneous glacial till–sandy aquifer system, *J. Hydrol.*, *243*(3–4), 162–179.

Nolan, B. T., R. W. Healy, P. E. Taber, K. Perkins, K. J. Hitt, and D. M. Wolock (2007), Factors influencing ground-water recharge in the eastern United States, *J. Hydrol.*, *332*, 187–205.

O'Leary, G. J. (1996), The effects of conservation tillage on potential groundwater recharge, *Agric. Water Manage.*, *31*(1–2), 65–73.

Petheram, C., G. Walker, R. Grayson, T. Thierfelder, and L. Zhang (2002), Towards a framework for predicting impacts of land-use on recharge: 1: A review of recharge studies in Australia, *Aust. J. Soil Res.*, *30*(3), 397–417.

Plummer, L. N. (2005), Dating of young groundwater, in *Isotopes in the Water Cycle: Past, Present and Future of a Developing Science*, edited by P. Aggarwal, J. Gat, and K. O. Froehlich, pp. 193–218, Springer, Netherlands.

Ritzi, R. W., D. F. Dominic, A. J. Slesers, C. B. Greer, E. C. Reboulet, J. A. Telford, R. W. Masters, C. A. Klohe, J. L. Bogle, and B. P. Means (2000), Comparing statistical models of physical heterogeneity in buried-valley aquifers, *Water Resour. Res.*, *36*(11), 3179–3192.

Rockhold, M. L., M. J. Fayer, C. T. Kincaid, and G. W. Gee (1995), Estimation of natural ground water recharge for the performance assessment of a low-level waste disposal facility at the Hanford site, *PNL-10508*, Batelle Pac. Northwest Natl. Lab., Richland, Wash.

Rundquist, D. C., A. J. Peters, L. Di, D. A. Rodekohr, R. L. Ehrman, and G. Murray (1991), Statewide groundwater-vulnerability assessment in Nebraska using the DRASTIC/GIS model, *Geocarto Int.*, *2*, 51–58.

Sanford, W. (2002), Recharge and groundwater models: An overview, *Hydrogeol. J.*, *10*, 110–120.

Sanford, W. (2011), Calibration of models using groundwater age, *Hydrogeol. J.*, *19*(1), 13–16.

Santoni, C. S., E. G. Jobbágy, and S. Contreras (2010), Vadose zone transport in dry forests of central Argentina: Role of land use, *Water Resour. Res.*, *46*, W10541, doi:10.1029/2009WR008784.

Scanlon, B. R. (2000), Uncertainties in estimating water fluxes and residence times using environmental tracers in an arid unsaturated zone, *Water Resour. Res.*, *36*(2), 395–409.

Scanlon, B. R., and R. S. Goldsmith (1997), Field study of spatial variability in unsaturated flow beneath and adjacent to playas, *Water Resour. Res.*, *33*(10), 2239–2252.

Scanlon, B. R., R. W. Healy, and P. G. Cook (2002), Choosing appropriate techniques for quantifying groundwater recharge, *Hydrogeol. J.*, *10*(1), 18–39.

Scanlon, B. R., R. C. Reedy, and J. A. Tachovsky (2007), Semiarid unsaturated zone chloride profiles: Archives of past land use change impacts on water resources in the southern High Plains, United States, *Water Resour. Res.*, *43*, W06423, doi:10.1029/2006WR005769.

Scanlon, B. R., C. C. Faunt, L. Longuevergne, R. C. Reedy, W. M. Alley, V. L. McGuire, and P. B. McMahon (2012), Groundwater depletion and sustainability of irrigation in the US High Plains and Central Valley, *Proc. Natl. Acad. Sci. U.S.A.*, *109*(24), 9320–9325.

Sebol, L. A., W. D. Robertson, E. Busenberg, L. N. Plummer, M. C. Ryan, and S. L. Schiff (2007), Evidence of CFC degradation in groundwater under pyrite-oxidizing conditions, *J. Hydrol.*, *347*(1–2), 1–12.

Seyfried, M., S. Schwinning, M. Walvoord, W. Pockman, B. Newman, R. Jackson, and F. Phillips (2005), Ecohydrological control of deep drainage in arid and semiarid regions, *Ecology*, *86*(2), 277–287.

Simmers, I. (1997), Groundwater recharge principles, problems and developments, in *Recharge of Phreatic Aquifers in (Semi-) Arid Areas*, edited by I. Simmers, pp. 1–18, A. A. Balkema, Rotterdam, Netherlands.

Stadler, S., K. Osenbrück, W. H. M. Duijnisveld, M. Schwiede, and J. Böttcher (2010), Linking chloride mass balance infiltration rates with chlorofluorocarbon and SF6 groundwater dating in semi-arid settings: Potential and limitations, *Isot. Environ. Health Stud.*, *46*(3), 312–324.

Stanton, J. S., S. L. Qi, D. W. Ryter, S. E. Falk, N. A. Houston, S. M. Peterson, S. M. Westenbroek, and S. C. Christenson (2010), Selected approaches to estimate water-budget components of the high plains, 1940 through 1949 and 2000 through 2009, *U.S. Geol. Surv. Sci. Invest. Rep. 2011–5183*, 79 pp.

Steele, G. V. (2002), Age of ground water at City of Lincoln's municipal well field near Ashland, Nebraska, *U.S. Geol. Surv. Sci. Invest. Rep. 2002-091*, 6 pp.

Sukhija, B. S., and C. R. Shah (1976), Conformity of groundwater recharge rate by tritium method and mathematical modeling, *J. Hydrol.*, *30*, 167–178.

Szilagyi, J., and J. Jozsa (2012), MODIS-aided statewide net groundwater-recharge estimation in Nebraska, *Ground Water*, *51*(6), 945–951, doi: 10.1111/j.1745-6584.2012.01019.

Szilagyi, J., V. Zlotnik, J. Gates, and J. Jozsa (2011), Mapping mean annual groundwater recharge in the Nebraska Sand Hills, USA, *Hydrogeol. J.*, *19*(8), 1503–1513.

Szilagyi, J., V. A. Zlotnik, and J. Jozsa (2012), Net recharge vs. depth to groundwater relationship in the Platte River Valley of Nebraska, United States, *Ground Water*, *51*(5), 735–744.

Troldborg, L., K. H. Jensen, P. Engesgaard, J. C. Refsgaard, and K. Hinsby (2008), Using environmental tracers in modeling flow in a complex shallow aquifer system, *J. Hydrol. Eng.*, *13*(11), 1037–1048.

Tyler, S. W., J. B. Chapman, S. H. Conrad, D. P. Hammermeister, D. O. Blout, J. J. Miller, M. J. Sully, and J. M. Ginanni (1996), Soil-water flux in the Southern Great Basin, United States: Temporal and spatial variations over the last 120,000 years, *Water Resour. Res.*, *32*(6), 1481–1499.

van Genuchten, M. Th. (1980), A closed form equation for predicting the hydraulic conductivity of unsaturated soils, *Soil Sci. Soc. Am. J*, *44*, 892–898.

van Genuchten, M. Th., F. J. Leij, and S. R. Yates (1991), The RETC code for quantifying the hydraulic functions of unsaturated soils, *Rep. EPA/600/2–91/065*, R. S. Kerr Environ. Res. Lab., U.S. Environ. Prot. Agency, Ada, Okla.

Vogel, J. C. (1967), Investigation of groundwater flow with radiocarbon, in *Isotopes in Hydrology*, pp. 355–368, Int. At. Energy Agency, Vienna.

Weissmann, G. S., Y. Zhang, E. M. LaBolle, and G. E. Fogg (2002), Dispersion of groundwater age in an alluvial aquifer system, *Water Resour. Res.*, *38*(10), 1198, doi:10.1029/2001WR000907.

Wilson, G. B., and G. W. McNeill (1997), Noble gas recharge temperatures and the excess air component, *Appl. Geochem.*, *12*(6), 747–762.

Xu, D., and A. Mermoud (2003), Modeling the soil water balance based on time-dependent hydraulic conductivity under different tillage practices, *Agric. Water Manage.*, *63*(2), 139–151.